HHS Public Access

Author manuscript

Otol Neurotol. Author manuscript; available in PMC 2017 December 01.

Published in final edited form as:

Otol Neurotol. 2016 December ; 37(10): 1541–1548. doi:10.1097/MAO.0000000000001232.

Intracochlear pressure transients during cochlear implant electrode insertion

Nathaniel T. Greene, PhD[a,b,*], **Jameson K. Mattingly, MD**[a], **Renee M. Banakis Hartl, AuD, MD**[a], **Daniel J. Tollin, PhD**[a,b], and **Stephen P. Cass, MD, MPH**[a]

[a]Department of Otolaryngology, University of Colorado School of Medicine, Aurora, CO

[b]Department of Physiology and Biophysics, University of Colorado School of Medicine, Aurora, CO

Abstract

Hypothesis—Cochlear implant (CI) electrode insertion into the round window induces pressure transients in the cochlear fluid comparable to high intensity sound transients.

Background—Many patients receiving a CI have some remaining functional hearing at low frequencies, thus devices and surgical techniques have been developed to utilize this residual hearing. To maintain functional acoustic hearing, it is important to retain function of any hair cells and auditory nerve fibers innervating the basilar membrane; however, in a subset of patients, residual low frequency hearing is lost following CI insertion. Here, we test the hypothesis that transient intracochlear pressure spikes are generated during CI electrode insertion, which could cause damage and compromise residual hearing.

Methods—Human cadaveric temporal bones were prepared with an extended facial recess. Pressures in the scala vestibuli (P_{SV}) and tympani (P_{ST}) were measured with fiber-optic pressure sensors inserted into the cochlea near the oval and round windows while CI electrodes (five styles from two manufacturers) were inserted into the cochlea via a round window approach.

Results—P_{ST} tended to be larger in magnitude than P_{SV}, consistent with electrode insertion into the scala tympani. CI electrode insertion produced a range of pressure transients in the cochlea that could occur alone or as part of a train of spikes with equivalent peak sound pressure levels in excess of 170dB SPL. Instances of pressure transients varied with electrode styles.

Conclusions—Results suggest electrode design, insertion mechanism, and surgical technique affect the magnitude and rate of intracochlear pressure transients during CI electrode insertion. Pressure transients showed intensities similar to those elicited by high level sounds and thus could cause damage to the basilar membrane and/or hair cells.

Keywords

Cochlear implant; electroacoustic stimulation; intracochlear pressures; hearing preservation

[*]Nathaniel T. Greene, Department of Physiology and Biophysics, University of Colorado School of Medicine, 12800 E. 19th Ave., Rm 7401G, Aurora, CO 80045, United States, Tele: 303-724-0637, Fax: 303-724-1961, nathaniel.greene@ucdenver.edu.

Conflict of Interest Statement:

Stephen P. Cass is a consultant on the Surgical Advisory Board for Cochlear Corporation.

Introduction

Cochlear implantation successfully improves speech perception in patients with cochlear hair cell loss via direct electrical stimulation of the auditory nerve. Recently, CIs have become available that are designed to work in conjunction with acoustical stimulation for patients with residual low frequency hearing (1–3). In some patients, however, that residual hearing is lost either immediately, or sometime after implantation (4). Additionally, injury to the vestibular organs (5), and resulting deficits in vestibular function (6), have been reported following CI implantation in 0.33–75% of patients (7–9).

Several mechanisms could contribute to these immediate deficits, including both conductive loss resulting from alterations to inner ear mechanics or cochlear impedance, and sensorineural loss resulting from direct trauma to cochlear structures and/or inflammation and cell death related to the electrode presence (10–16). The causes of these deficits are not currently known.

A sensorineural hearing loss immediately following electrode insertion could result from electrode contact with the basilar membrane, but another intriguing possibility is that the electrode insertion force generates large pressures in the cochlear fluid thus stimulating the cochlea ‘acoustically’ (17). A series of recent papers reported intracochlear pressure changes for several speeds of electrode insertions (via a linear actuator) (18), and different insertion techniques (19) in an artificial cochlear model. Mean maximal intracochlear pressures were reported up to 170 Pa, or ~140 dB SPL peak; however, no large transients were observed, possibly because these studies were conducted in an artificial cochlea model. No intracochlear pressure measurements have been reported in human temporal bones to the best of our knowledge. To overcome this knowledge gap, here we report intracochlear pressure recordings in cadaveric human temporal bones made during insertion of several commercially available cochlear implant electrodes.

Methods

Thirteen ears in fresh-frozen whole or hemicephalic heads with intact temporal bones and no history of middle ear disease were evaluated (Lone Tree Medical, Littleton, CO, USA). The use of cadaveric human tissue was in compliance with the University of Colorado Anschutz Medical Campus Institutional Biosafety Committee (COMIRB EXEMPT #14-1464). Responses were assessed in whole-head specimens immediately following tests studying the mechanisms of bone-conducted hearing (20).

Temporal Bone Preparation

A detailed description of the temporal bone preparation has appeared previously (16,20), and were similar to methods described previously by our laboratory (21–23), as well as other authors (24). Briefly, specimens were thawed in warm water, a canal-wall-up mastoidectomy and extended facial recess approach was performed, and the cochlear promontory was thinned near the oval and round windows. Figure 1 shows the facial recess exposure from one specimen (427L). Cochleostomies into the scala tympani (ST) and scala vestibuli (SV)

were created, after blue-lining the cochlear promontory (Figure 1A), using a fine pick under a droplet of water (Fig. 1B). Commercially available, off-the-shelf fiber-optic pressure sensors (FOP-M260-ENCAP, FISO Inc., Quebec, QC, Canada), similar to those used in several recent studies in our lab and elsewhere (16, 20, 25), were inserted (Fig. 1C), and sealed with alginate dental impression material (Jeltrate; Dentsply International Inc., York, PA). Pressure probe placements and approximate location of the basilar membrane were verified after each experiment by dissecting out the cochlear promontory bone between the two cochleostomy sites (Fig. 1D). Note: it was not always possible to differentiate individual components of the cochlear partition, such as the basilar membrane or the spiral lamina; however, manipulation with a pick verified that it was soft tissue and not bony - hereafter we refer to this partition simply as the basilar membrane. Out-of-plane velocity of the stapes (VStap) was measured with a single-axis LDV (OFV-534 & OFV-5000; Polytec Inc., Irvine, CA) mounted to a dissecting microscope (Carl Zeiss AG, Oberkochen, Germany). Microscopic retro-reflective glass beads (P-RETRO 45–63 μm dia., Polytec Inc., Irvine, CA) were placed on the neck and posterior crus of the stapes to ensure a strong LDV signal since the stapes footplate was typically obscured by the presence of the stapes tendon. Velocity measurements are not presented in this report.

Cochlear Implant Electrode Insertion

Cochlear implant (CI) electrodes were inserted by Otolaryngology residents under the guidance of Neurotology faculty. The speed of electrode insertion was not precisely controlled in order to simulate the natural variation of insertion speeds the senior author has observed in CI surgeons, and typically occurred over about 10 seconds. Electrodes were inserted into the cochlea underwater through a cochleostomy made in the round window (RW) with a fine pick. CI electrodes were inserted using an insertion tool and/or a pair of fine forceps. CI electrodes used in these experiments were: Nucleus Hybrid L24 (HL24; Cochlear Ltd, Sydney, Australia), Nucleus CI422 Slim Straight inserted to 25 mm (SS20 & SS25; Cochlear Ltd, 95 Sydney, Australia), Nucleus CI24RE Contour Advance (NCA; Cochlear Ltd, Sydney, Australia), HiFocus Mid-Scala (MS; Advanced Bionics AG, Stäfa, Switzerland), and HiFocus 1J (1J; Advanced Bionics AG, Stäfa, Switzerland). Electrode dimensions are provided in table 1 and are the same as those studied in Greene et al. (16). Electrodes were inserted sequentially, under water, into the ST via a RW approach (Fig. 1C), and were generally inserted in the order listed above and Table 1. The cochleostomy was sealed following each electrode insertion with alginate dental impression material, and excess water was removed via suction from the middle ear cavity following insertion.

Sound Presentation, Data Acquisition, and Data Analysis

All experiments were performed in a double-walled sound-attenuating chamber (IAC Inc., Bronx, NY). Sound stimuli were generated, and responses recorded as described previously (16,20). Briefly, stimuli were generated digitally, presented to the specimen closed-field magnetic speaker (MF1; Tucker-Davis Technologies Inc., Alachua, FL) powered by one channel of a stereo amplifier (SA1), and driven by an external sound card (Hammerfall Multiface II, RME, Haimhausen, Germany). Baseline acoustic transfer functions were generated from presentation of short tone pips between 100 and 12000 Hz. Input from the microphone, LDV, and pressure sensors were simultaneously captured via the sound card

analog inputs. Signals acquired during implant insertion were band-pass filtered between 1 – 250 Hz with a second order Butterworth filter.

Statistical analyses were completed using functions in the Statistics and Machine Learning toolbox in Matlab (R2014b; The Mathworks Inc., Natick, MA, USA). Differences in pressures across electrodes and measurement locations (i.e. P_{SV}, P_{ST}, or P_{Diff}) were assessed with a two-way anova (the "anovan" function), and post hoc testing performed with a Tukey-Kramer HSD (honest significant difference) test (the "multcompare" function). Correlations between pressure magnitude and electrode characteristics was performed using the "corrcoef" function. Statistical comparisons are assessed at the $\alpha = 0.05$ unless otherwise specified.

Results

Acoustic closed-field transfer functions

Stapes velocity (V_{Stap}) and intracochlear pressures (P_{IC}) were assessed prior to making the RW cochleostomy in order to verify the condition of each temporal bone. Baseline closed-field acoustic transfer functions ($H_{Stap/RW/SV/ST/Diff}$) from a subset of these specimens have been reported previously (16,20). One specimen (427R) showed an H_{Stap} consistently outside the range of responses previously reported for healthy temporal bones (27), thus was excluded from further analysis. Responses collected from the remaining specimens were consistent with previous reports (24–28).

Intracochlear pressure transients

Figure 2 shows example P_{IC} recordings as a function of time in one specimen (8948R) during insertion of the SS25 electrode array. Figure 2A shows P_{SV} (light gray), and P_{ST} (dashed, dark gray) for the 30 s recording duration. The approximate duration of the electrode insertion is marked with a horizontal bar, began ~2 s after the start of the recording, was ~ 10 s in duration, and complete at ~ 12 s. A series of large pressure transients are visible starting at approximately 5 seconds in both P_{IC} recordings, and are shown in greater detail in figure 2B, which also includes the differential intracochlear pressure ($P_{Diff} = P_{SV} – P_{ST}$; black). In each of the seven transients observed during this insertion, P_{ST} shows somewhat higher magnitude pressure transients than P_{SV}, consistent with the close proximity of the P_{ST} recording probe with the CI electrode insertion site. The largest transient (shown in figure 2C) showed a peak pressure magnitude of ~ 600 Pa, or ~150 dB (referenced to 20μPa) in the P_{ST} recording, with a corresponding P_{SV} magnitude of ~ 400 Pa (~146 dB referenced to 20μPa). Two smaller transients are visible at approximately 19 s and at 29 s, after completion of the insertion. These transients occur only (or primarily) in the P_{ST} channel, suggesting that these events are artifacts generated by manipulation of the pressure probe by the CI electrode in the cochlea, the experimenter contacting the pressure probe, or the experimenter applying Jeltrate to the round window membrane to seal the round window membrane cochleostomy after electrode insertion.

P_{SV} is typically larger than P_{ST}, thus P_{Diff} is generally positive for acoustic stimulation. In contrast, cochlear implant electrodes are inserted into scala tympani, thus the peaks in P_{ST}

are generally larger than P_{SV}, and consequently the peaks of the pressure transients are P_{Diff} observed can be negative. In the example shown, P_{ST} showed larger peak magnitudes, but since the peaks were negative, the P_{Diff} observed was positive. Additionally, the pressure transient is somewhat delayed in P_{SV} compared to P_{ST}, thus the magnitude of the transient in P_{Diff} is somewhat larger (up to ~300 Pa in this example; Fig. 2C) than would be expected from a simple comparison of the peak pressures observed in P_{SV} and P_{ST}.

Equivalent Ear Canal SPL

The pressures observed in the cochlea can be directly related to sound in the earcanal via the acoustic transfer function. In order to estimate the sound pressure level (SPL) in the external auditory canal (EAC) that would have elicited an intracochlear pressure matching the measured pressure, we generated a 128-tap finite impulse response (FIR) filter from the inverse of the mean acoustic transfer function for each signal observed previously in healthy human temporal bones (16,24) using the Matlab function *fir2*. Figure 3 shows the result of applying these filters to the signals shown in Figure 2. The EAC SPL (in Pa) estimate derived from P_{ST} shows comparable magnitudes to the original P_{ST} recordings, consistent with the low gain observed in the P_{ST}/P_{EAC} transfer function. Similarly, the EAC SPL estimate from both P_{SV} and P_{Diff} are both lower in magnitude than the recorded pressures shown in Figure 2 due to the ear canal resonance and middle ear gain observable in the P_{SV}/P_{EAC} and P_{Diff}/P_{EAC} transfer functions (24). P_{ST} produces a larger EAC SPL estimate than P_{SV} and P_{Diff}, which are comparable in magnitude but opposite in sign compared to one another.

Maximum pressures due to CI insertion observed across recordings

In order to compare recordings, the absolute peak pressures were found in each recording using the *findpeaks* Matlab function. Peaks were constrained to a minimum peak height of 4x the standard deviation within each recording, a minimum peak spacing of 10 ms. Furthermore, peaks were only assessed if peaks occurred within 1 ms of one another in both P_{SV} and P_{ST}, or P_{Diff} and P_{ST} in order to avoid inclusion of artifacts such as those visible late in the recordings shown in Figs. 2A & 3A. The absolute maximum peak pressures observed in all recordings in all specimens, in all electrodes tested, are summarized in Figure 4, where Fig. 4A shows the maximum peak pressures in the estimated EAC SPL (dB SPL peak), and Fig. 4B the unfiltered recorded pressures. Peak pressures are shown from 14 recordings with the HL24, 25 recordings with the SS25, 13 recordings with the MS, 11 recordings with the NCA, and 7 recordings with the 1J. Individual peaks are shown as gray shaded circles, and the median (± 25%) for each condition is represented by boxplots (the full range of responses is represented with the whiskers, and outliers indicated by a +). In general, pressures observed during CI insertion varied between ~ 100 Pa, which roughly corresponded with the peak pressure threshold in most recordings, and ~10 kPa. These pressure levels correspond to approximately a 134–174 dB SPL sound in the EAC SPL estimate, suggesting that CI electrode insertion can produce pressure transients in the cochlea comparable in magnitude to those that would be produced by high intensity sound presented to the ear.

A two-way analysis of variance (ANOVA) was performed with peak pressures (dB re 20 μPa) as the dependent variable, and electrode and recording location as independent variables, for both unfiltered and estimated EAC SPL conditions. Results for the unfiltered pressures (Fig. 4B) reveal a main effect of electrode ($F_{4,108} = 4.29$; $p = 0.003$), but not recording location ($F_{2,108} = 1.11$; $p = 0.33$) or the interaction ($F_{8,108} = 0.45$; $p = 0.89$). Post hoc Tukey honest significant difference (hsd) pairwise comparisons reveal significant differences between the 1J and: HL24 ($p = 0.003$), SS25 ($p = 0.006$), and MS ($p = 0.01$). Conversely, results for the estimated EAC SPLs (Fig. 4A) reveal a main effect of recording location ($F_{2,80} = 5.03$; $p = 0.009$), but not electrode ($F_{2,80} = 1.63$; $p = 0.176$) or the interaction ($F_{8,80} = 0.40$; $p = 0.92$). Post hoc Tukey hsd pairwise comparisons reveal significant differences between the EAC SPL estimate from P_{ST} is significantly different than from both P_{SV} ($p = 0.028$) and P_{Diff} ($p = 0.014$).

Discussion

Comparison to Prior Investigations

To the best of our knowledge, no prior reports of transient intracochlear pressures generated during CI electrode insertion exist. However, a number of studies have used similar techniques to assess several different aspects of insertion on the cochlea. Forces encountered during insertion have been assessed for a number of years, in particular used to compare insertion techniques (e.g. (29,30)) and electrode designs (e.g. (31)). While not explicitly investigating the phenomenon, one study reported that insertion by hand (compared to via a robot) resulted in lower overall pressures, but with a greater likelihood of generating intermittent peaks (30), comparable to the events generated in the current results.

Intracochlear pressures generated in a plastic model cochlea have been measured (using similar techniques and sensors to the current study) more recently in a series of reports by Roland (17), and Todt and colleagues. These studies investigated the effects of insertion speed (18), insertion technique (i.e. unsupported, supported, or automated) (19), and size of the opening in the round window (32), each revealing generation of large static pressures (~ 200 Pa, or 140 dB SPL) during the insertion. It is interesting that no transient pressures are reported; however this may be due to the use of a plastic model, compared to cadaveric temporal bones in this study. Regardless, the magnitude of pressures generated are comparable, highlighting the risk of transient pressure generation during CI electrode insertion.

Source of Intracochlear Pressure Transients

These results reveal that pressure transients may be relatively common during CI electrode insertion. Several different sources of these events could arise during electrode insertion; however, these results provide little evidence as to the source of these transients. Nevertheless a number of potential sources seem likely to contribute. First, translocation of the CI electrode array from the ST to the SV, resulting from a puncture of the cochlear partition by the electrode array, could produce a large transient pressure event (33), and is known to occur in a subset (perhaps up to ~30% (34)) of patients; however, such a source is unlikely to produce a train of transients as observed in Fig. 2, since translocation of the

electrode multiple times appears unlikely and uncommon (35). Second, transients could be generated should the electrode array contact either the basilar membrane (e.g. lifting observed in histological studies (36)), or the outer wall of the cochlear duct. A prior study suggested that frictional forces between the electrode and the outer wall was responsible for a large proportion of the force encountered during electrode insertion for straight (but perhaps not pre-curved) electrode arrays; however, no hydraulic forces were observed in this prior study, suggesting this is an unlikely source of these transients (17). Third, variability in the size and shape of the opening made in the RW membrane may affect intracochlear pressures, as a small cochleostomy will resist outflow of cochlear fluid displaced by the electrode array more than a large cochleostomy (32). Furthermore, this impedance would result in a relatively slow build-up followed by a transient release of pressure during insertion, repeated over and over until insertion was complete, thus could generate a train of transient events during insertion.

Evidence for this final possibility is visible in the slight, but significant, variations in peak pressures observed across electrode styles. There was not a strong relationship between observed peak pressures and electrode style, as straight electrodes showed both the highest and lowest pressure ranges observed, whereas perimodiolar electrodes (MS & NCA) were in the middle (note however, that the 1J is pre-curved, but not to the extent of the MS or NCA). Similarly, there is not a strong relationship between electrode length, nor apical diameter (see table 1), and median peak SPLs observed ($R^2 < 0.6$, $p > 0.13$). In contrast, peak pressure *was* strongly associated with basal diameter and electrode volume (V, estimated as the volume of a conical frustum: $V = 1/3 * h * (R_1^2 + R_1R_2 + R_2^2)$, where h = electrode length, R_1 = basal diameter/2, and R_2 = apical diameter/2) for P_{ST} ($R^2 = 0.94$ & 0.95, $p = 0.017$ & 0.015 respectively), but not P_{SV} or P_{Diff} ($R^2 < 0.78$, $p > 0.12$). These relationships indicate that intracochlear pressure transient magnitudes are affected by electrode designs, where large fluid displacement, or a large basal diameter (which may increase resistance to fluid flow out of the cochleostomy), increases the magnitude of peak pressures generated.

One additional possibility is that some proportion of the observed events were artifacts of mechanical contact between the electrode array and the pressure transducer tip inserted within the scala tympani, or with the experimenter and a portion of the pressure transducer outside of the cochlea. Indeed, such events were likely common during the course of this series of experiments due to the proximity of the scala tympani pressure probe to the electrode. To minimize the impact that these questionable events on the results we require coincident pressure transients in P_{SV} and P_{ST} for inclusion in the analysis, which would be unlikely to occur except via fluid conduction.

Overall, while the current results cannot discriminate between the potential sources of these pressures transients, it is likely that these events arise by some combination of mechanical contact between the CI electrode array and the cochlea, as well as via hydromechanical forces interacting with the round window membrane. Additional experiments are required in order to determine the sources of the pressures generated during CI electrode array insertion and to assess effects of insertion speeds on pressures in human temporal bones.

Equivalent Acoustic Transient Exposure

In this study we sought to characterize the peak pressures observed in the cochlea during cochlear implant insertion. Our results suggest that intracochlear pressure transients were produced that correspond to equivalent ear canal sound pressure levels of up to ~ 174 dB SPL peak, which matches the range of sound intensities that are produced from modern small arms fire (measured 1 m from the shooter)(37,38) and low level blast exposure. It is important to note that the Occupational Safety & Health Administration standard states that "Exposure to impulsive or impact noise should not exceed 140 dB peak sound pressure level" with no regard to the frequency content of the sound (39).

While the absolute peak pressures observed due to CI insertion were comparable to those produced by small arms fire, the time-course and related frequency content of these events is somewhat different. Small arms fire tends to produce relatively short acoustic transients with relatively high frequency content (e.g. Murphy and Tubbs observed maximum energy between 500–800 Hz in most firearms, and at higher frequencies in the remainder)(37), whereas blast exposure can produce much larger SPLs, depending upon the proximity of the listener to the source.

The period of the example transients shown in Figs. 2 and 3 is ~ 0.2 s, suggesting a peak in the frequency spectrum near ~ 5 Hz, which are typical of shock waves generated by an explosive blast and recorded in the free field (40). The intracochlear pressure acoustic transfer functions have not been characterized at these extremely low frequencies, thus the estimated EAC SPL values reported may be inaccurate. However, preliminary data from our lab suggests that the transfer function gain is low (near zero) or negative for low frequency and high intensity sound. These results are comparable in gain to the lowest frequencies tested in prior reports (16,24), suggesting that the EAC SPL estimates are reasonable.

Blast exposure often results in complaints of otalgia, tinnitus, aural fullness, dizziness, loudness sensitivity, distorted hearing, and hearing impairment, indicative of damage to both the auditory and vestibular end organs (41). The effects of blast injury to auditory and vestibular function have been thoroughly described (41,42); however, the mechanisms underlying that injury are not well characterized. While injury to the external and middle ear structures is unlikely during CI electrode insertion, symptoms related to a sensorineural hearing and vestibular loss could result from hair cell loss in response to the high sound pressure levels. Importantly, any injury resulting from a pressure transient would be compounded by additional damage resulting from mechanical trauma to the basilar membrane as well as conductive losses (16).

Limitations

Despite the relatively straightforward nature of the results, a number of factors limit the extent to which the results of this study can be generalized. First, although the specimens included were more complete than an excised temporal bone, the condition of the tissue could have been compromised due to tissue degradation. In particular, the presence and patency of the cochlear aqueduct, which may act to regulate perilymphatic pressure (43,44), could not be verified. Second, and related, we did not perform histology on the specimens

after implantation, so we do not know the precise trajectory of CI electrode inside the cochlea. In particular, we are unable to assess the amount of mechanical damage to the cochlear partition, up to and including translocation of the electrode into the scala vestibuli, occurred during the experiment. Furthermore, we are unable to correlate anatomical features with the pressures observed, thus the discussion of the origin of these pressure transients remains speculative. Finally, the large pressures observed in this study suggest that hair cell loss in both the auditory (which is relatively common (45)) and vestibular systems should be expected; however, CI patients exhibiting these symptoms are seldom observed in the clinic. This disparity may result from a number of factors including: the transient nature of the pressures observed here, which are generally less damaging than an ongoing noise of comparable level; pre-existing hearing loss, which may mask new hearing loss; and the fact that vestibular injury is only seldom observed following blast exposure (46).

Conclusions

Cochlear implantation has the potential to profoundly improve patient quality of life, particularly in cases where residual low frequency hearing can be retained following implantation. However, electrode insertion into the cochlea can potentially cause loss of this residual hearing in a number of ways. First, insertion can cause substantial damage to tissue in the cochlea directly, including the basilar membrane, via mechanical trauma. Second, the presence of the electrode, or an immune response to the presence of the electrode, could cause a conductive hearing loss. Finally, we have demonstrated here that a transient pressure wave resulting from electrode insertion could be of a sufficiently high amplitude (up to 174 dB SPL) as to cause injury to the auditory system. These results suggest that surgeons should prioritize the use of ‘soft’ techniques, and electrode designers should prioritize ‘silent’ design, to minimize the generation of these acoustical transients.

Acknowledgments

Funding:

Funding was provided by NIH/NIDCD: 1T32-DC012280 (NTG).

References

1. Gantz BJ, Turner CW. Combining acoustic and electrical hearing. Laryngoscope. 2003; 113:1726–30. [PubMed: 14520097]
2. von Ilberg C, Kiefer J, Tillein J, et al. Electric-acoustic stimulation of the auditory system. New technology for severe hearing loss. ORL J Otorhinolaryngol Relat Spec. 1999; 61:334–40. [PubMed: 10545807]
3. Turner CW, Gantz BJ, Vidal C, et al. Speech recognition in noise for cochlear implant listeners: benefits of residual acoustic hearing. J Acoust Soc Am. 2004; 115:1729–35. [PubMed: 15101651]
4. Balkany TJ, Connell SS, Hodges AV, et al. Conservation of residual acoustic hearing after cochlear implantation. Otology & Neurotology. 2006; 27:1083–8. [PubMed: 17130798]
5. Handzel O, Burgess BJ, Nadol JB Jr. Histopathology of the peripheral vestibular system after cochlear implantation in the human. Otology & Neurotology. 2006; 27:57–64. [PubMed: 16371848]
6. Chen X, Chen X, Zhang F, et al. Influence of cochlear implantation on vestibular function. Acta Oto-Laryngologica. 2016:1–5.

7. Enticott JC, Tari S, Koh SM, et al. Cochlear implant and vestibular function. Otol Neurotol. 2006; 27:824–30. [PubMed: 16936568]
8. Vibert D, Hausler R, Kompis M, et al. Vestibular function in patients with cochlear implantation. Acta Otolaryngol Suppl. 2001; 545:29–34. [PubMed: 11677737]
9. Kubo T, Yamamoto K, Iwaki T, et al. Different forms of dizziness occurring after cochlear implant. European archives of oto-rhino-laryngology: official journal of the European Federation of Oto-Rhino-Laryngological Societies. 2001; 258:9–12.
10. Eshraghi AA. Prevention of cochlear implant electrode damage. Current opinion in otolaryngology & head and neck surgery. 2006; 14:323–8. [PubMed: 16974145]
11. Chole RA, Hullar TE, Potts LG. Conductive component after cochlear implantation in patients with residual hearing conservation. Am J Audiol. 2014; 23:359–64. [PubMed: 25165991]
12. Lenarz T, Stover T, Buechner A, et al. Temporal bone results and hearing preservation with a new straight electrode. Audiol Neurootol. 2006; 11(Suppl 1):34–41. [PubMed: 17063009]
13. Tamir S, Ferrary E, Borel S, et al. Hearing preservation after cochlear implantation using deeply inserted flex atraumatic electrode arrays. Audiol Neurootol. 2012; 17:331–7. [PubMed: 22813984]
14. Usami S, Moteki H, Suzuki N, et al. Achievement of hearing preservation in the presence of an electrode covering the residual hearing region. Acta Otolaryngol. 2011; 131:405–12. [PubMed: 21208024]
15. Raveh E, Attias J, Nageris B, et al. Pattern of hearing loss following cochlear implantation. European Archives of Oto-Rhino-Laryngology. 2014:1–6.
16. Greene NT, Mattingly JK, Jenkins HA, et al. Cochlear Implant Electrode Effect on Sound Energy Transfer Within the Cochlea During Acoustic Stimulation. Otol Neurotol. 2015; 36:1554–61. [PubMed: 26333018]
17. Roland JT Jr. A Model for Cochlear Implant Electrode Insertion and Force Evaluation: Results with a New Electrode Design and Insertion Technique. Laryngoscope. 2005; 115:1325–39. [PubMed: 16094101]
18. Todt I, Middmann P, Ernst A. Intracochlear Fluid Pressure Changes Related to the Insertion Speed of a CI Electrode. BioMed Res Int. 2014
19. Todt I, Ernst A, Mittmann P. Effects of Different Insertion Techniques of a Cochlear Implant Electrode on the Intracochlear Pressure. Audiol Neurotol. 2016; 21(30)
20. Mattingly JK, Greene NT, Jenkins HA, et al. Effects of Skin Thickness on Cochlear Input Signal Using Transcutaneous Bone Conduction Implants. Otol Neurotol. 2015; 36:1403–11. [PubMed: 26164446]
21. Deveze A, Koka K, Tringali S, et al. Active middle ear implant application in case of stapes fixation: a temporal bone study. Otol Neurotol. 2010; 31:1027–34. [PubMed: 20679957]
22. Lupo JE, Koka K, Jenkins HA, et al. Vibromechanical Assessment of Active Middle Ear Implant Stimulation in Simulated Middle Ear Effusion: A Temporal Bone Study. Otology & Neurotology. 2014; 35:470–5. [PubMed: 23988990]
23. Tringali S, Koka K, Deveze A, et al. Round window membrane implantation with an active middle ear implant: a study of the effects on the performance of round window exposure and transducer tip diameter in human cadaveric temporal bones. Audiol Neurootol. 2010; 15:291–302. [PubMed: 20150727]
24. Nakajima HH, Dong W, Olson ES, et al. Differential intracochlear sound pressure measurements in normal human temporal bones. J Assoc Res Otolaryngol. 2009; 10:23–36. [PubMed: 19067078]
25. Grossöhmichen M, Salcher R, Püschel K, Lenarz T, Maier H. Differential Intracochlear Sound Pressure Measurements in Human Temporal Bones with an Off-the-Shelf Sensor. BioMed Res Int. 2014
26. Rosowski JJ, Chien W, Ravicz ME, et al. Testing a method for quantifying the output of implantable middle ear hearing devices. Audiol Neurootol. 2007; 12:265–76. [PubMed: 17406105]
27. Stenfelt S, Hato N, Goode RL. Round window membrane motion with air conduction and bone conduction stimulation. Hear Res. 2004; 198:10–24. [PubMed: 15567598]
28. Stenfelt S, Hato N, Goode RL. Fluid volume displacement at the oval and round windows with air and bone conduction stimulation. J Acoust Soc Am. 2004; 115:797–812. [PubMed: 15000191]

29. Todd C, Naghdy F, Svehla MJ. Force Application During Cochlear Implant Insertion: An Analysis for Improvement of Surgeon Technique. IEEE Trans Biomed Eng. 2007; 54:1247–55. [PubMed: 17605356]
30. Majdani O, Schurzig D, Hussong A, et al. Force Measurement of insertion of cochlear implant electrode arrays in vitro: comparison of surgeon to automated insertion tool. Acta Otolaryngol. 2010; 130:31–6. [PubMed: 19484593]
31. Adunka O, Kiefer J, Unkelbach MH, et al. Development and evaluation of an improved cochlear implant electrode design for electric acoustic stimulation. The Laryngoscope. 2004; 114:1237–41. [PubMed: 15235353]
32. Todt I, Ernst A, Mittmann P. Effects of Round Window Opening Size and Moisturized Electrodes on Intracochear Pressure Related to the Insertion of a Cochlear Implant Electrode. Audiol Neurotol. 2016; 6:1–8.
33. Schuster D, Kratchman LB, Labadie RF. Characterization of intracochlear pressure rupture forces in fresh human cadaveric cochleae. Otol Neurotol. 2015; 36:657–61. [PubMed: 25233332]
34. Aschendorf A, Kromeier J, Klenzner T, Laszig R. Quality control after insertion of the Nucleus Contour and Contour Advance Electrode in Adults. Ear & Hearing. 2007; 28:75S–79S. [PubMed: 17496653]
35. Finley CC, Skinner MW. Role of electrode placement as a contributor to variability in cochlear implant outcomes. Otology & neurotology: official publication of the American Otological Society, American Neurotology Society [and] European Academy of Otology and Neurotology. 2008 Oct.29(7):920.
36. Adunka O, Unkelbach MH, MacK M, Hambek M, Gstoettner W, Kiefer J. Cochlear implantation via the round window membrane minimizes trauma to cochlear structures: a histologically controlled insertion study. Acta oto-laryngologica. 2004 Sep 1; 124(7):807–12. [PubMed: 15370564]
37. Murphy WJ, Tubbs RL. Assessment of noise exposure for indoor and outdoor firing ranges. Journal of occupational and environmental hygiene. 2007; 4:688–97. [PubMed: 17654224]
38. Keim RJ. Impulse noise and neurosensory hearing loss. Relationship to small arms fire California medicine. 1970; 113:16–9. [PubMed: 5460217]
39. [Accessed April 20, 2016] OSHA Standard 29 CFR 1910.25(b)(2). Available at: https://www.osha.gov/dts/osta/otm/noise/standards.html
40. Reed JW. Atmospheric attenuation of explosion waves. The Journal of the Acoustical Society of America. 1977; 61:39–47.
41. Fausti SA, Wilmington DJ, Gallun FJ, et al. Auditory and vestibular dysfunction associated with blast-related traumatic brain injury. The Journal of Rehabilitation Research and Development. 2009; 46:797. [PubMed: 20104403]
42. Patterson JH Jr, Hamernik RP. Blast overpressure induced structural and functional changes in the auditory system. Toxicology. 1997; 121:29–40. [PubMed: 9217313]
43. Carlborg B, Densert B, Densert O. Functional patency of the cochlear aqueduct. Annals of Otology, Rhinology & Laryngology. 1982 Mar 1; 91(2):209–15.
44. Gopen Q, Rosowski JJ, Merchant SN. Anatomy of the normal human cochlear aqueduct with functional implications. Hearing research. 1997 May 31; 107(1):9–22. [PubMed: 9165342]
45. Gstoettner W, Helbig S, Settevendemie C, et al. A new electrode for residual hearing preservation in cochlear implantation: first clinical results. Acta oto-laryngologica. 2009 Jan 1; 129(4):372–9. [PubMed: 19140036]
46. Remenschneider AK, Lookabaugh S, Aliphas A, et al. Otologic outcomes after blast injury: the Boston Marathon experience. Otology & Neurotology. 2014 Dec 1; 35(10):1825–34. [PubMed: 25393974]

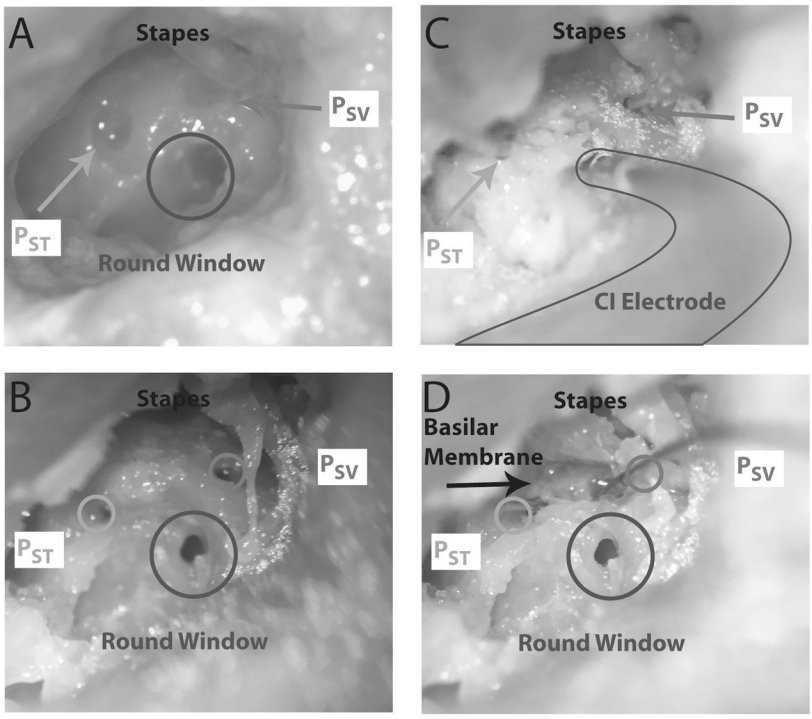

Figure 1.

Photomicrographs of the specimen (specimen 427L) preparation. A) Temporal bones are prepared with a mastoidectomy and facial recess. The scala vestibuli (SV) and scala tympani (ST) are blue lined near the oval and round windows in preparation for the intracochlear pressure probes. B) Cochleostomies are made in the cochlea in order to accept the pressure probes, a cochleostomy is made in the round window to accept the cochlear implant electrode, and retroreflective glass beads placed on the stapes for baseline LDV measurements. C) Fiber-optic pressure probes are inserted into the SV (P_{SV}) and ST (P_{ST}), and CI electrode inserted into the round window. All cochleostomies are sealed with dental impression material. D) The bone between the SV and ST cochleostomies is dissected away to reveal the location of the basilar membrane. Circles show the approximate location that P_{SV} and P_{ST} entered the cochlea.

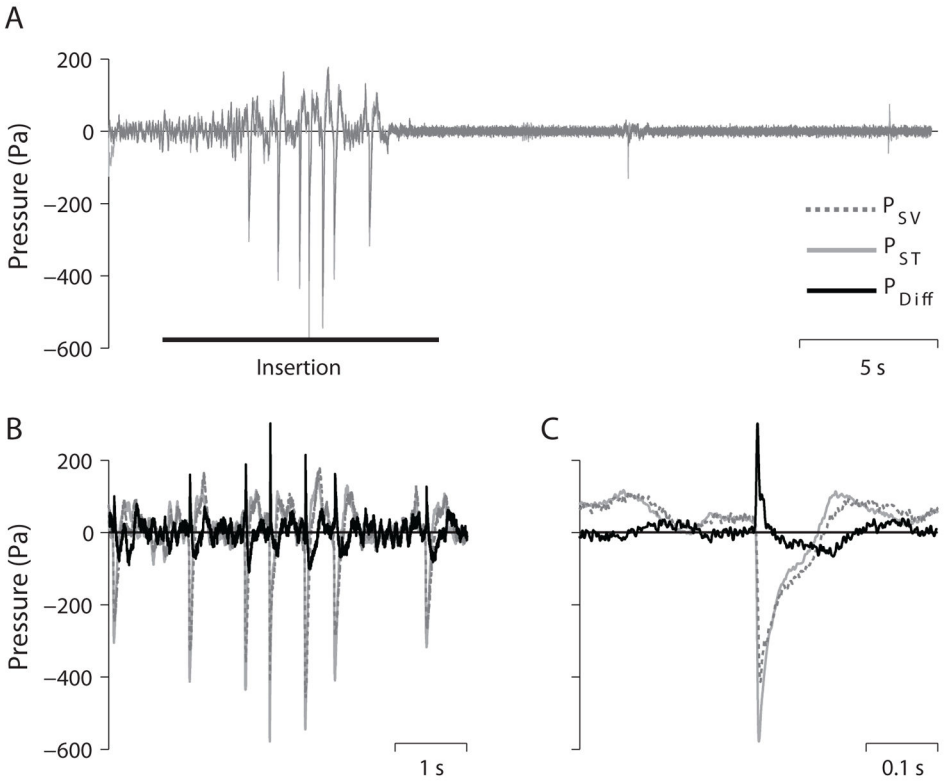

Figure 2.

Example intracochlear pressure recordings (specimen 8948R) shown for three different time scales. A) Scala vestibuli (P_{SV}), scala tympani (P_{ST}), and the differential pressure (P_{Diff} = ($P_{SV} - P_{ST}$)) for a 30 s long recording of a cochlear implant electrode insertion (SS25). Several transients are visible in all traces between 5–10 s (B). The largest transient (C) in all three traces occurs midway through this recording.

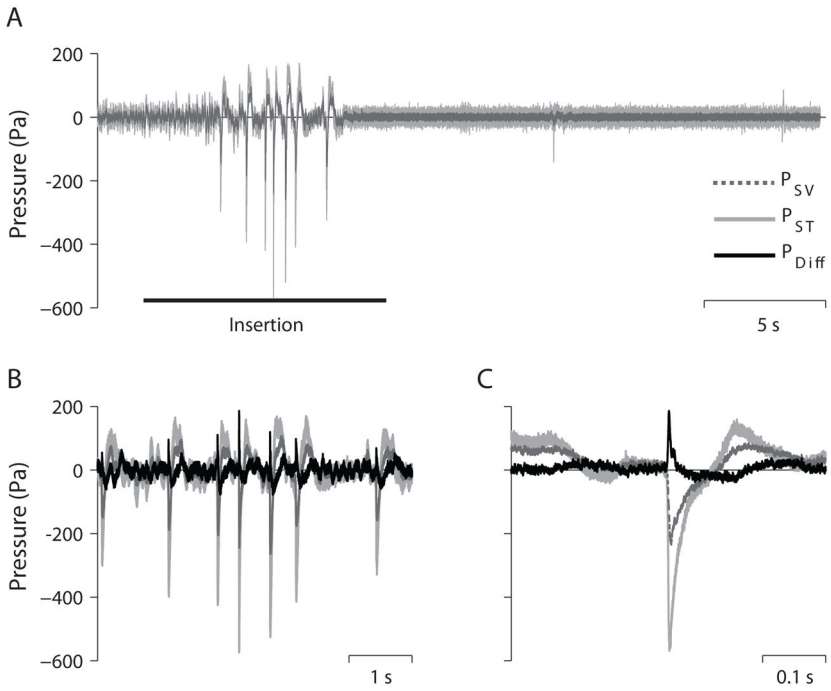

Figure 3.

Estimated equivalent ear canal sound pressure level. The same pressure traces shown in Fig. 2, reverse filtered with corresponding acoustic transfer functions in order to estimate the sound pressure level required in the EAC to produce the observed intracochlear sound pressure levels.

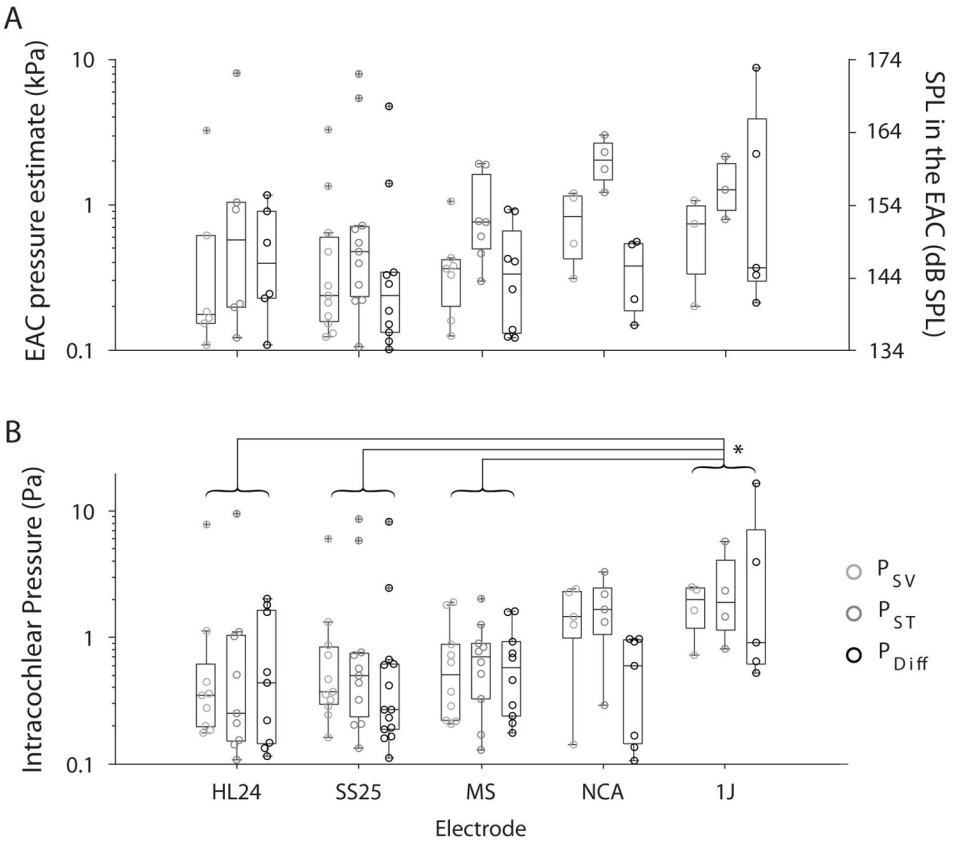

Figure 4.

Summary of peak sound pressure levels observed during all CI electrode insertions. A) Estimated EAC SPLs, and B) unfiltered peak intracochlear pressure measurements are shown for each pressure measurement (gray shaded circles), as a function of electrode style. Box plots represent the median ± 25% of the range of pressures observed, whiskers show the full range of the estimated distribution, and +'s represent outliers.

Table 1

Implant	Electrode Length	Basal diameter	Apical diameter	Tip diameter
Cochlear Nucleus Hybrid L24	16	0.4	0.25	n/a
Cochlear Nucleus Slim Straight CI422	20 and 25	0.6	0.3	n/a
AB HiFocus Mid-scala	18.5	0.7	0.5	n/a
Cochlear Nucleus CI24RE Contour advance	20	0.8	0.5	0.2
AB HiFocus 1J	25	0.8	0.4	n/a